Published in final edited form as:
J Proteome Res. 2008 October ; 7(10): 4384–4395. doi:10.1021/pr800376w.

Comprehensive Characterization of Heat Shock Protein 27 Phosphorylation in Human Endothelial Cells Stimulated by the Microbial Dithiole Thiolutin

Shujia Dai[†,‡], **Yifeng Jia**[‡,§], **Shiaw-Lin Wu**[†,‡], **Jeff S. Isenberg**[§], **Lisa A. Ridnour**[‖], **Russell W. Bandle**[§], **David A. Wink**[‖], **David D. Roberts**[§], and **Barry L. Karger**[*,†]

†*Barnett Institute, Northeastern University, Boston, Massachusetts 02115*

§*Laboratory of Pathology, Center for Cancer Research, National Cancer Institute, National Institutes of Health, Bethesda, Maryland 20892*

‖*Radiation Biology Branch, Center for Cancer Research, National Cancer Institute, National Institutes of Health, Bethesda, Maryland 20892*

Abstract

Thiolutin is a sulfur-based microbial compound with known activity as an angiogenesis inhibitor. Relative to previously studied angiogenesis inhibitors, thiolutin is a remarkably potent inducer of heat shock protein 27 (Hsp27) phosphorylation. This phosphorylation requires p38 kinase but is independent of increased p38 phosphorylation. To elucidate how thiolutin regulates Hsp27 phosphorylation and ultimately angiogenesis, Hsp27 was immunoprecipitated using nonphosphorylated and phospho-Ser78 specific antibodies from lysates of thiolutin treated and untreated human umbilical vein endothelial cells and analyzed by LC–MS. Separate LC–MS analyses of Lys-C, Lys-C plus trypsin, and Lys-C plus Glu-C digests provided 100% sequence coverage, including the identification of a very large 13 kDa Lys-C fragment using a special sample handling procedure (4 M guanidine HCl) prior to the LC–MS analysis to improve the large peptide recovery. The analysis revealed a novel post-translational modification of Hsp27 involving truncation of the N-terminal Met and acetylation of the penultimate Thr. Analysis of a Glu-C fragment containing two phosphorylation sites, Ser78 and Ser82, and a tryptic fragment containing the other phosphorylation site, Ser15, enabled quantitative stoichiometry of Hsp27 phosphorylation by LC–MS. The strategy revealed details of Hsp27 phosphorylation, including significant di-phosphorylation at both Ser78 and Ser82, that would be difficult to obtain by traditional approaches because oligomerization of the hydrophobic N-terminal region of the molecule prevents efficient enzymatic cleavage. The combination of Western blotting, immunoprecipation, and LC–MS provides a quantitative analysis of thiolutin-stimulated Hsp27 phosphorylation and further defines the role of Hsp27 in the antiangiogenic activities of thiolutin and related dithiolethiones.

Keywords

Hsp27; acetylation; phosphorylation; N-terminal cleavage; recovery of large peptides; label-free quantitation of PTMs; immunoprecipitation; LC–MS

*To whom correspondence should be addressed. E-mail: b.karger@neu.edu.
‡These authors contributed equally to this work.

Introduction

Hsp27 belongs to a family of small stress proteins that play diverse roles as chaperones and as regulators of cytoskeletal stability, cell motility, protein folding, and cellular stress and survival responses.[1–4] The oligomerization and functional activities of Hsp27 are regulated by phosphorylation of the protein. Nonphosphorylated Hsp27 exists primarily in an oligomeric state via N-terminal interactions, which reversibly dissociates into smaller oligomers and monomer following phosphorylation of the protein.[5–7] Physiological stimuli (redox signaling, cytokines, and growth factors) and various forms of stress dramatically increase the phosphorylation of human Hsp27 at Ser15, Ser78, and Ser82 residues, which are essential for acquired tolerance of stress.

Hsp27 phosphorylation is a major regulator of cell motility. In migrating cells, nonphosphorylated Hsp27 localizes to the leading edge of lamellipodia, but phosphorylated Hsp27 appears to be excluded from this site.[8] Hsp27 was originally proposed to serve as an Actin capping protein, but recent evidence indicates that blocking Hsp27 phosphorylation impairs Actin assembly by sequestering Actin monomers.[9] These authors propose that Hsp27 facilitates Actin-based motility through a phosphorylation cycle that shuttles Actin monomers to regions of new Actin filament assembly. In human endothelial cells, inhibition of p38-MAPK activity abolishes Hsp27 phosphorylation while increasing Actin polymerization and cell migration.[5] On the other hand, phosphorylation of Hsp27 stabilizes the Actin cytoskeleton and decreases endothelial cell migration.[1,10]

Hsp27 phosphorylation involves several signal transduction pathways. MK2, one of the MAP kinase-activated protein (MAPKAP) kinases, is the dominant kinase mediating Hsp27 phosphorylation. When activated by p38 MAP kinase, MK2 phosphorylates human Hsp27 at Ser15, Ser78, and Ser82 *in vitro*[11–13] and is necessary for its phosphorylation *in vivo*.[14] Akt also plays an important role in Hsp27 phosphorylation. Akt can directly phosphorylate Hsp27 *in vitro*, which induces dissociation of Hsp27 from Akt.[15] p38 constitutively associates with Hsp27 in a MK2-dependent manner, but Hsp27 also associates with Akt independent of MK2.[16] Silencing Hsp27 using RNAi prevents Ser473 phosphorylation of Akt in human renal tubular cells and prevents MK2 interaction with Akt.[17] This suggests that an Akt/Hsp27/MK2 complex regulates signaling through p38. In addition, protein kinase D (formerly known as PKCμ) can phosphorylate Hsp27 at Ser82.[18] It is not known whether Ser15 and 78 on Hsp27 are also substrates for this kinase. Besides these three major serine phosphorylation sites, Hsp27 is phosphorylated at Thr143 by the cGMP-dependent protein kinases (cGK).[19]

Phosphorylation of Hsp27 alters its subcellular distribution between the cytoplasm and nucleus as well as within the cytoplasm.[20] A global proteomic analysis of endothelial cell signaling targets for four dissimilar angiogenesis inhibitors identified increased Hsp27 phosphorylation as a common response, and all inhibitors induced nuclear translocation of Hsp27.[10] Hsp27 phosphorylation was subsequently confirmed to be a target for additional angiogenesis inhibitors including endorepellin and some dithioles.[21,22] These results suggested that Hsp27 phosphorylation could potentially be a useful biomarker for development of therapeutic angiogenesis inhibitors. Several phospho-peptide antibodies have been developed to analyze Hsp phosphorylation, but these approaches provide only a qualitative assessment. A quantitative method has not yet been established to define the kinetics and stoichiometry of phosphorylation at each site in Hsp27.

The microbially derived dithiole thiolutin (*N*-(4-methyl-3-oxo-7,8-dithia-4-azabicyclo[3.3.0] octa-1,5-dien-2-yl)acetamide)[23] is known to inhibit tumor angiogenesis,[24] and increased phosphorylation of Hsp27 was found to be a conserved response of endothelial cells to at least seven other angiogenesis inhibitors.[10,21,22] We now report that thiolutin is an exceptionally

active member of this class of compounds for selectively inducing Hsp27 phosphorylation in endothelial cells. We report here a quantitative mass spectrometric analysis of thiolutin-stimulated Hsp27 phosphorylation in endothelial cells and show that this phosphorylation requires p38 but is not mediated by activation of this kinase. These studies demonstrate the advantage of analyzing large peptide fragments, an intermediate between intact proteins (top-down) and tryptic fragments (bottom-up), to improve the detection sensitivity with high sequence coverage including post-translational modifications (PTMs) of the targeted proteins.[25–27] Employing a novel sample handling procedure, we discovered a new PTM of Hsp27, namely truncation of N-terminal Met, followed by acetylation of subsequent Thr. In addition, since both non-phosphorylated and phosphorylated forms could be quantified in the same LC–MS analysis, the stoichiometry of Hsp27 phosphorylation could be estimated. The methodology offers the potential to improve the understanding of post-translational regulation of Hsp27 and may facilitate the therapeutic application of these sulfur-based compounds to control pathological angiogenesis.

Materials and Methods

Reagents

Human umbilical vein endothelial cells (HUVEC), endothelial cell basal medium (EBM), and fetal calf serum (FCS) were obtained from Cambrex (Walkersville, MD). Eosin methylene blue (EMB) was from Gemini Bio (Woodland, CA), and anethole-dithiolethione (5-[*p*-methoxyphenyl]-3H-1,2-dithiol-3-thione, ADT) was a gift from Milan University. 3H-1,2-dithiole-3-thione (D3T) was purchased from LKT Laboratories (St. Paul, MN), while anti-Hsp27 antibody and Hsp27 phosphorylation specific antibodies (Ser15, 78, and 82) were from Millipore (Billerica, MA). NP40, TWEEN-20, and protease inhibitor cocktail-I were obtained from EMD Biosciences (La Jolla, CA). Thiolutin, monoclonal human anti-CD31 antibody, bovine serum albumin (BSA), phosphatase inhibitor cocktails I and II, sodium fluoride, sodium orthovanadate, citrate, beta-mercaptoethanol (BME), dithiothreitol (DTT), iodoacetamide (IAA), guanidine hydrochloride, and ammonium bicarbonate were purchased from Sigma (St. Louis, MO). Paramagnetic protein A Dynabeads, NuPage protein gel reagents (4 × lithium dodecyl sulfate [LDS] sample buffer, Novex Bis-Tris protein gels, MOPS and MES SDS running buffers, transfer buffer, and antioxidant), Invitrolon 0.45 μm PVDF, and SYPRO Ruby gel stain were obtained from Invitrogen (Carlsbad, CA), and ECL Plus enhanced chemiluminescence kit was from GE Healthcare (Piscataway, NJ). Carnation nonfat dry milk (NFDM) was from Nestle USA (Solon, OH), and endoprotease Lys-C from Wako (Richmond, VA). Formic acid, acetone and acetonitrile were purchased from ThermoFisher (Watham, MA), and HPLC-grade water used in all experiments was from J.T. Baker (Bedford, MA).

Cell Culture and Thiolutin Treatment

HUVEC were maintained in endothelial cell growth medium, containing the manufacturer's additives and 2.5% FCS, and grown in a 5% CO_2 atmosphere at 37 °C. Cells were utilized between passages 4–8. Purity of cultures was monitored by immunochemical staining with monoclonal human anti-CD31 antibody. Proliferation of HUVEC was measured using a nonradioactive colorimetric assay (CellTiter 96, Promega, Madison, WI). Briefly, to each well of a 96-well culture plate (Nunc, Denmark), 5×10^3 cells suspended in 100 μL of endothelial cell growth medium were added and incubated in the presence of the indicated treatment agents for 72 h at 37 °C in 5% CO_2. Appropriate zero time controls were run for all assays, and the optical density readings were subtracted from those obtained at 72 h to calculate net cell proliferation. HUVEC were treated by replacing the medium with warmed EBM 0.1% BSA containing 1 μM thiolutin and incubating for 1 h at 37 °C.

Cell Lysis

Immediately following stimulation, the HUVEC cells were washed 3 times with ice-cold TBS and lysed on ice with 5 mL of modified radioimmunoprecipitation (RIPA) buffer (50 mM Tris-HCl, pH 7.4, 150 mM NaCl, 1% NP40, 1× protease inhibitor cocktail set I, and 1X phosphatase inhibitor cocktail sets I and II) per plate for 5 min, scraped, and then transferred to a 50 mL tube. Pooled lysates from untreated or treated samples were adjusted to 50 mL with additional RIPA buffer, followed by 5 passages through a 21-gauge needle, incubation on ice for 30 min, and finally centrifugation at 10 000× g for 10 min. The clarified supernatants were transferred to new 50 mL tubes and normalized by total protein concentration using micro BCA assay (ThermoFisher).

Immunoprecipitation (IP)

Mouse IgG and antibodies against Hsp27 and Hsp27-P78 (Upstate) were cross-linked to Dynabeads coated with protein G (DPG, Invitrogen) following the manufacturer's instructions. HUVEC were lysed in RIPA-0.5% NP-40 (150 mm plate/mL RIPA). After centrifugation, the supernatant was collected for IP. Preclearance was performed by adding 100 μL of DPG-IgM per mL HUVEC lysate and incubating at RT for 30 min with gentle mixing. DPG-IgG was pulled down and washed 3 times with PBS 0.01% Tween 20 by magnetic separation. The DPG-IgG-bound proteins were eluted into 200 μL of 0.1 M citrate (pH 2–3) at RT for 2 min. The elution process was repeated 2 times (total 600 μL), and then 300 μL of 50 mM Tris pH 9.5 was added to the eluted sample to neutralize the citrate. The supernatant, after preclearance, was collected and divided equally for antibody immunoprecipitation using a ratio of 100 μL of DPG-Hsp27 or DPG-Hsp27-P78 per mL of the supernatant. The reactions were incubated at RT for 60 min with gentle mixing. The beads were collected and washed 3 times with PBS, 0.01% Tween by magnetic separation. The DPG-Hsp27- or DPG-Hsp27-P78-bound protein (s) were eluted as described above, and the samples were stored at −80 °C for Western blotting and mass spectrometric analysis.

Western Blot Analysis

HUVEC were starved overnight in EBM + 1% FCS and then treated with the reagents at the indicated dosages and duration. Cells were washed, collected by centrifugation, and lysed by 1× SDS sample buffer containing 1× protease inhibitors. After centrifugation, the protein extract was separated by SDS-PAGE and transferred to an Immobilon-P membrane (Millipore) via semidry transfer apparatus (Bio-Rad, Hercules, CA) according to the manufacturers' instructions. Membranes were blocked with 5% nonfat dry milk at RT for 1 h and incubated with primary antibodies overnight at 4 °C. After three washes with DPBS, the membranes were incubated with secondary antibodies (Jackson ImmunoResearch, West Grove, PA) at room temperature for 1 h and followed by five washes with DPBS. The reacting bands were detected using enhanced chemiluminescence (ThermoFisher). Membranes were then reprobed with antiactin antibody for sample loading control.

Multiple Enzymatic Digestions

After immunoprecipitation, proteins eluted from the cross-linked antibody/protein-G beads were buffer exchanged with 6 M guanidine hydrochloride using a Microcon ultracentrifuge device (10 kDa MWCO; Millipore) for 5 cycles (10 000× g for 5 min per cycle). The exchanged protein solution was reduced with 20 mM DTT for 30 min at 37 °C and alkylated with 50 mM of IAA in the dark at RT for 1.5 h. After buffer exchange, endoproteinase Lys-C (1:100 w/w) was added to digest the protein for 4 h at 37 °C. The Lys-C digests were split into three equal aliquots. One aliquot was used directly for LC–MS analysis, one was digested a second time by trypsin (1:50, w/w), and the final one digested a second time by endoprotease Glu-C (1:40 w/w). In each case, digestion was halted by addition of formic acid to a final concentration of

1%, and then the solution was concentrated down to ~10 μL. Approximately 2 μL of the digest was directly loaded onto the LC column for LC–MS analysis. The reminder of the sample was stored at −80 °C for further use.

LC–MS

LC–MS experiments were performed on an LTQ-FTMS instrument (ThermoFisher) with an Ultimate 3000 nano-LC pump (Dionex, Mountain View, CA) using a C-8 reversed phase column (75 μm i.d. × 10 cm, 5 μm particle size, 300 Å pore size, Vydac C8, Grace Davison, Deerfield IL) or a monolithic column (polystyrene divinylbenzene, 50-μm inner diameter × 10 cm), which was prepared in-house.[26] Mobile phase A was 0.1% formic acid in water, and mobile phase B was 0.1% formic acid in acetonitrile. The gradient used for all analyses was: (i) 40 min at 0% B for sample loading, (ii) linear gradient to 40% B over 40 min, then (iii) to 80% B over 10 min, and finally (iv) constant 80% B for 10 min. The flow rate of the column was set at 200 nL/min for the C8 column and at 100 nL/min for the monolithic column. The experimental parameters of the LTQ-FT mass spectrometer and the acquisition modes for MS2 and MS3 were similar to those in our previous study.[24] Briefly, the mass spectrometer was operated in the data-dependent mode to switch automatically between MS, MS2, and MS3 acquisitions. Survey full scan MS spectra with two microscans (*m*/*z* 400–2000) were acquired in the FTICR cell with mass resolution of 100,000 at *m*/*z* 400 (after accumulation to a target value of 2×10^6 ions in the linear ion trap) followed by four cycles of sequential MS2 and MS3 scans. Dynamic exclusion was utilized with an exclusion duration of 30 s and 2 repeat counts. Selected reaction monitoring (SRM), which measured specific fragment ions in the MS/MS mode, was used if a given peptide had multiple phosphorylation sites with the same mass (e.g., phosphorylation at either pS78 or pS82), and the phosphorylated peptides were not well separated by LC. In the SRM mode, the mass spectrometer was set to acquire the FTICR MS scan, followed by a targeted MS/MS scan on a particular *m*/*z* ion (average of 2 microscans) in the linear ion trap within a given retention time window. The specific ions in the MS/MS spectra were used to differentiate the phosphorylation sites. Similarly, a targeted MS3 scan was utilized for further confirmation of the site of phosphorylation. The peak areas of the phosphopeptide ions, either from the MS spectra (XIC) or the MS^2 or the MS^3 spectra (SRM), were extracted for quantitation (i.e., phosphopeptides) or normalization (i.e., nonphosphorylated counterparts).

Peptide Assignment

The assignments of peptides (for charge state ≤3+), large peptides (for charge state ≥4+), and phosphopeptides were similar to our previous report.[25] Briefly, the Sequest algorithm in the BioWorks software (version 3.3.2, ThermoFisher) was used to search all MS^2 and MS^3 spectra against spectra of theoretical fragmentations (b and y ions) of a human Swiss-Prot annotated database, downloaded in Jan 2007 (14,194 protein entries), with a mass tolerance of ± 1.4 Da without any enzymatic specificity. The resultant spectra were filtered using the scores of Xcorr (1+ precursor ion ≥1.5, 2+ ≥ 2.0, and 3+ ≥ 2.5) and with semienzymatic specificity, containing either Lys-C plus trypsin or Lys-C plus Glu-C specificity. Peptides (≤3+ ions) were assigned with a probability greater than 95% confidence and the mass accuracy of the precursor ions of less than 5 ppm. Since no rigorous statistics are available for peptides with ≥4+ charges, Sequest was used to select and rank the most probable peptides, and the top assignment was further confirmed by the mass accuracy of the precursor ion (<5 ppm) and the preferred fragmentation patterns in the observed MS^2 and MS^3 spectra. For Hsp27 phosphopeptides, the data were searched against a single database corresponding to the sequence of Hsp27 with the parameter of differential modification (Ser, Thr, and Tyr) equal to +80 Da. The locations of the phosphorylated sites in the identified phosphopeptides were further confirmed by manual inspection of related b and y ions.

Results

Thiolutin was previously shown to potently inhibit endothelial cell adhesion (IC_{50} <1 μM) as well as to inhibit S180 tumor-induced angiogenesis in mice.[27] The mechanism by which thiolutin inhibits endothelial cell adhesion and angiogenesis was not clear, but two focal adhesion proteins were affected by the microbial compound treatment. Specifically, thiolutin inhibited the phosphorylation of focal adhesion kinase (FAK) and reduced the expression of paxillin in HUVEC plated on vitronectin. Because we recently found that two structurally related dithiolethiones have antiangiogenic activity and induce phosphorylation of Hsp27,[22] we considered that thiolutin might have a similar mode of action. These structurally related dithiolethiones and thiolutin are compared in the next section, followed by a detailed LC–MS analysis of Hsp27.

Endothelial Cell Proliferation Is Potently and Selectively Inhibited by Thiolutin

Of the three dithiole-compounds tested, thiolutin was clearly the most potent, dramatically inhibiting HUVEC proliferation at 0.1 μM, whereas D3T was only effective at 100 μM and ADT had only minimal effects on HUVEC proliferation (Figure 1A). The potent antiproliferative activity of thiolutin was selective for endothelial cells in that several other tumor cell lines showed weaker inhibition of proliferation by thiolutin (i.e., at 10 μM), and a small cell lung carcinoma cell line was completely resistant (Figure 1B). Thus, thiolutin appeared to be a selective inhibitor of endothelial cell proliferation.

Thiolutin is a Potent Stimulator of Hsp27 Phosphorylation

Of the three dithiole compounds, thiolutin was the most potent for inducing Hsp27 phosphorylation (Figure 2A). Based on Western blotting using three Hsp27 phosphorylation sitespecific antibodies, treatment with 1 μM thiolutin stimulated time-dependent Hsp27-phosphorylation, particularly at S78. Significant phosphorylation at S82 was also detected at 30 and 60 min, and weak and transient phosphorylation of S15 was observed. D3T at 1 μM stimulated phosphorylation of S78, but to a much less extent than thiolutin. In contrast, ADT, at the same concentration, had almost no effect on Hsp27 phosphorylation (Figure 2A). Actin was used as a housekeeping protein control to normalize the protein amounts (Figure 2A).

To define further the effect of thiolutin on Hsp27 phosphorylation at S78, we conducted a dose and time course study of the pS78 of Hsp27 in response to the thiolutin treatment. (Figure 2B). From the Western blots, it can be seen that thiolutin induced the pS78 of Hsp27 in a dose and time dependent manner. The kinetics of phosphorylation varied with thiolutin concentration over a concentration range from 0.1 to 100 μM, and phosphorylation could be maintained for up to 24 h (data not shown). At 0.1 μM thiolutin, pS78 was detected in one hour after treatment with a maximum response at 3 h, while at 0.5 μM, the pS78 could be detected within 30 min, increasing up to 5 h, followed by a slow decline.

The above studies demonstrate that inhibition of HUVEC proliferation correlated with the phosphorylation of Hsp27 by thiolutin, particularly, at S78 (compare Figure 2A with Figure 1A). To determine if the pS78 of Hsp27 by thiolutin is specific for HUVEC, several other cell lines exposed to different concentrations of thiolutin were tested (Figure 2C). All of the tumor cell lines tested exhibited less robust Hsp27 phosphorylation responses to 0.5 μM thiolutin than HUVEC. In particular, OH-1 small cell lung carcinoma cells showed no Hsp27 expression or phosphorylation response. Similar to the inhibition of cell proliferation, as described in Figure 1, the potent activity of low dose thiolutin to phosphorylate Hsp27 appeared to be relatively selective for HUVEC as well. These results further support using HUVEC to study thiolutin induced Hsp27 phosphorylation.

p38 is Required for Hsp27 Phosphorylation but Is Not Activated by Thiolutin

MK2, when activated by p38 MAP kinase, is the principal kinase that phosphorylates Hsp27, and activation of the p38 pathway has been reported by other redox stress responses.[3] Thus, we further examined whether thiolutin activates this MAP kinase pathway to increase downstream Hsp27 phosphorylation.

At 10 μM, thiolutin significantly increased ERK and JNK phosphorylation but neither p38 phosphorylation nor the MAP kinase phosphatase (MKP-1) were enhanced (Figure 3A). The ERK response was also unlikely to mediate the increased Hsp27 phosphorylation because no ERK phosphorylation was seen at lower thiolutin concentrations (≤1 μM) that were sufficient to induce maximum Hsp27 phosphorylation. Only JNK phosphorylation was observed in HUVEC treated with 1 μM thiolutin (Figure 3A). This result suggested that JNK could mediate Hsp27 phosphorylation. However, Hsp27 phosphorylation by 1 μM thiolutin was not prevented by the JNK inhibitor SP600125 (Figure 3B). In contrast, Hsp27 phosphorylation was diminished in the presence of a p38 inhibitor. As shown in Figure 3C, the treatment of HUVEC with the p38 inhibitor SB203680 in a dose-dependent manner inhibited pS78 of Hsp27 stimulated by 0.5 μM thiolutin. Near complete inhibition was achieved using a dose of 40 μM for 20 min (the fifth lane in Figure 3C), and no Hsp27 phosphorylation was found in the control without thiolutin (the last lane in Figure 3C). Thus, thiolutin-induced Hsp27 phosphorylation required p38 (Figure 3C). However, thiolutin must act downstream of p38 to increase Hsp27 phosphorylation because it did not increase p38 phosphorylation.

Activation of the p38/MK2 pathway stimulates Hsp27 phosphorylation at all three serine residues (S15, S78, and S82),[9,11,13,14] but, as seen above, Western blotting does not permit quantitative analysis or comparison of the efficiency of phosphorylation at these three serine residues. To assess further the site specificity of Hsp27 phosphorylation induced by thiolutin, we developed a quantitative analysis of Hsp27 phosphorylation using mass spectrometry.

Characterization of Immunoprecipitated Hsp27 by LC–MS

Based in Figure 2A, 1 μM thiolutin induced optimal phosphorylation of Hsp27 (i.e., pS78) in HUVEC at 60 min. Thus, immunoprecipitation (IP) of Hsp27 from HUVEC, treated with thiolutin at 1 μM for 60 min along with the control (no treatment) was selected for characterization of Hsp27 phosphorylation using LC–MS analysis. Two cell lysates (with and without thiolutin treatment at 1 μM for 60 min) were subjected to IP using an antibody specific for the C-terminal end of the backbone of Hsp27 and, separately, a second antibody specific for phosphorylation at S78. Thus, a total of four IP samples were obtained for subsequent LC–MS analysis (Figure 4A). Each sample was first digested by endoprotease Lys-C, which yielded a large fragment from the N-terminal of Hsp27 with a molecular weight of 13 kDa (1–112 in Figure 5). A further enzymatic digestion was performed to obtain shorter peptide fragments, and the subsequent digests (by trypsin or Glu-C) were analyzed by nano-HPLC coupled to an LTQ-FTMS (Figure 4B). The identified peptides are summarized in Figure 5A and 5B. As shown in the figures, the Lys-C plus trypsin-digested peptides were identified with 89.3% sequence coverage, and the Lys-C plus Glu-C digested peptides with 63.9% sequence coverage. Combining these two analyses, a high sequence coverage of 96% was achieved, including the identification of all 3 phosphorylation sites. A peptide containing the pS15 site was identified in the sample from Lys-C plus trypsin digest, and a peptide containing both pS78 and pS82 modifications was identified from the Lys-C plus Glu-C digest.

Even though 96% sequence coverage of Hsp27 was obtained, the expected N-terminal peptide was not observed using the above strategy. One explanation could be that the N-terminal peptide (i.e., MTER) is too small to be observed following this double enzyme treatment. However, the initial 60 amino acids from the N-terminus (except for MTER), which were not

observed in the Lys-C plus Glu-C digest, were detected with low intensity in the Lys-C plus trypsin digest. Another reason could be the hydrophobic nature at the N-terminal region of the molecule, prone to oligomerization *via* N-terminal interactions, as mentioned in the introduction,[6,10] prevented efficient enzymatic cleavages in this region. Thus, the Lys-C-only digest, which yielded a cleavage at residue 112, was explored in the following steps.

Figure 6A shows the base ion chromatogram of the Lys-C digest. The largest Lys-C peptide fragment was eluted at 37.14 min. The successful observation of this large fragment (13 kDa) was a result of the addition of 4 M guanidine hydrochloride to the sample after digestion (see Discussion section). Multiple charges for this peptide (11+ to 19+) were observed by FTICR MS (Figure 6B). The peptide precursor ion with the highest charge state (14+) and the highest *m*/*z* 907.9143 with a well-resolved isotopic pattern are shown in the insert of Figure 6B. To our surprise, the molecular weight of this precursor ion did not match the expected molecular weight of the 1–112 peptide fragment. However, the molecular weight of this precursor ion matched that of an acetylated 2–112 peptide fragment, subtracting the molecular weight of methionine from the N-terminus and adding 42.0101 Da for acetylation. To confirm this hypothesis, fragmentation of this precursor ion was next examined. Since the charge state of this precursor ion was very high (i.e., 14+), the product ions of the CID-MS^2 fragmentation were analyzed in the FTICR MS (Figure 6C). As seen in the insert of Figure 6C, one of the most intense fragment ions was y66 with a 7+ charge state. The fragment ions in the Figure 6C all indicated that N-terminal threonine (penultimate to the originally N-terminal Met) was acetylated. One of the small MS^2 fragment ions (i.e., b16 with 3+ charge) was further targeted for fragmentation in the MS^3 step to confirm that the acetylation modification was indeed at the N-terminal Thr (Figure S1 in the Supporting Information).

To our knowledge, there has been no literature report of Hsp27 acetylation. However, the Met-Thr sequence found in Hsp27 is frequently cut by methionine amino peptidase in *Escherichia coli* proteins,[28] and acetylation of another heat shock protein (Hsp70) has been reported.[29] N-terminal acetylation can protect intracellular proteins from proteolysis,[30] thus preventing further truncation of the primary structure of Hsp27. It should also be noted that we only observed this des-Met and acetylated Hsp27 (i.e., 100%), and no other forms at N-terminus of Hsp27 were observed. Although phosphorylated Hsp27 preferentially localizes to the nucleus,[5,8–10] the cellular location of this des-Met and acetylated Hsp27 at the N-terminus has not been determined. However, several reports described phosphorylated and N-terminal acetylated peptides in yeast mitochondria,[31] the binding of acetylation enzymes with AT-Pase in mitochondria,[32] the cross talk between nuclear and mitochondrial genomes,[33] and this may suggest trafficking of Hsp27 through mitochondria where aminopeptidase cleavage and acetylation action can take place. After the identification of this modified N-terminal sequence (from residues 2 to 112), 100% sequence coverage was achieved for Hsp27.

Phosphorylation of Hsp27

The strategy for identification and quantitation of phosphorylation sites was similar to our previous studies[24,25] using the accurate precursor mass measurement provided by the FTMS (within 5 ppm) with the product ions of the expected cleavages in the CID-MS^2 and CID-MS^3 spectra. The identification of peptide fragment 65–87 containing pS82 is used to illustrate the approach. The base ion chromatogram of the Lys-C plus Glu-C digest is shown in Figure 7A. The peptide fragment of 65–87 containing pS82 was eluted at 43.43 min. The peptide precursor ion with the charge state of 3+ and the highest isotopic *m*/*z* 795.7603 was observed by FTICR MS (Figure 7B). The CID-MS^2 fragmentation of this precursor ion was automatically acquired in the ion trap by data-dependent acquisition (Figure 7C). As shown in

Supporting Information Available: Figure S1–S7. This material is available free of charge via the Internet at http://pubs.acs.org.

Figure 7C, the three most intense ions were y19, y19 with the neutral loss of phosphoric acid, and the precursor ion with the neutral loss of phosphoric acid. All three ions were automatically selected by data-dependent acquisition for CID-MS^3 fragmentation. Fragmentation of the y19 with the neutral loss of phosphoric acid yielded further evidence of the phosphorylation location as shown in Figure 7D. The site of phosphorylation, pS82, was identified by the observation of y5, b13, and b14 ions in the MS^2 spectrum (insert of Figure 7C). Related fragmentation of the peptide with a neutral loss at pS82 (b13 and b14 ions) were also identified in the MS^3 spectrum (Figure 7D), further confirming the assignment.

Using MS^2 and MS^3 fragmentation, we also identified the monophosphorylated (pS78) and the doubly phosphorylated (pS78 + pS82) peptides in the same LC–MS run at a slightly different retention time (Figure S7 in the Supporting Information). In addition to identification, the extracted ion chromatogram (XIC) from the MS^2 or MS^3 fragmentation could be used for quantitation as well. The XIC using the ion (*m*/*z* 966.7) from the MS^3 fragmentation is shown in Figure 8, in which the 966.6 ion was generated from the fragmentation of the ion (*m*/*z* 1015.6) and the 1015.6 ion from the MS^2 fragmentation of the precursor ion (*m*/*z* 795.7). As shown, the XIC of pS78 mono-phosphorylated peptide eluted at a retention time of 42.96 min, and the XIC of pS82 monophosphorylated peptide at 43.43 min (Figure 8A). The relative amount of the phosphorylated forms were also compared using different antibodies for the IP of Hsp27 (Figure 8A and B). Similarly, the XIC of the double phosphorylated peptide (pS78 + pS82), eluting at the retention time of 43.22 min, could be used for comparison as well (Figure S7 in the Supporting Information). Only a trace amount of pS15 phosphopeptide was found in the Lys-C plus trypsin digest (data not shown). No additional phosphorylation sites (e.g., Thr143) were found in this set of experiments. The detailed characterization of pS15, pS78, pS82, and pS78 + pS82 peptides to pinpoint the phosphorylation locations is shown in the Supporting Information (Figure S2– S6).

While Western blotting is a useful tool to screen the desired proteins, quantitation with multiple modifications could be difficult (e.g., pS78 antibody could not differentiate the protein with pS78 from the protein with both pS78 and pS82 modifications). In this study, in addition to singly phosphorylated forms, the diphosphorylation (pS78 + pS82) of Hsp27 was clearly observed by mass spectrometry. Thus, the phosphorylation population (stoichiometry), which has been determined by LC–MS approach with a different protein in our previous report,[24] was further examined in the following.

Estimated Stoichiometry for Hsp27 Phosphorylation

Once the phosphopeptide was identified, the precursor mass of the phosphopeptide and its nonphosphorylated counterpart were extracted, and the peak area of each extracted ion chromatogram (XIC) was used for quantitation. Since the various forms of a given peptide fragment were observed in the same run, we have used the estimated stoichiometry (ES) as a quantitative measure of the extent of phosphorylation at each site, as described previously.[24] The %ES was obtained from the peak area of the measured phosphopeptide (e.g., pS82) divided by the sum of all forms of the given peptide (e.g., pS78 + pS82 + [pS78 + pS82] + nonphosphorylated peptide). The % ES of various phosphorylation forms of Hsp27 is shown in Table 1. Consistent with the Western blot results (Figure 2A), phosphorylated forms of Hsp27 could be only detected in the thiolutin-treated samples, pS78 and pS82 dramatically higher as compared to the untreated control. IP of Hsp27 using the antibody against the C-terminal end yielded pS82 as the dominant form (47%) followed by the diphosphorylation of S78 and S82 (16%), and then the monophosphorylation of S78 (5%). IP using the antibody against pS78 yielded diphosphorylation of S78 and S82 as the major form (61%), followed by the roughly equivalent monophosphorylation of S78 (12%), and the monophosphorylation of S82 (10%). IP using the pS78 antibody indeed enhanced the pS78 form (Figure 7B), while IP

using the antibody against the C-terminal region of the protein showed that pS82 is more highly phosphorylated in response to thiolutin than pS78 (Figure 8A). However, the antibody against pS78 was not able to distinguish the pS78 form from that with both pS78 and pS82 phosphorylation (Figure S7 in the Supporting Information). A trace amount of pS15 was also found from the IP of the antibody against pS78 (less than 1%; data not shown), which mirrored the result of Western blot (1 μM thiolutin for 60 min in Figure 2A).

From these mass spectrometric analyses, the IP from the antibody against the C-terminal end of Hsp27 produced the dominant pS82 form, and the IP from the antibody against the pS78 region enriched mainly the forms containing pS78. In both cases, there were significant amounts of the diphosphorylation population, in addition to the individual population of pS78 or pS82 (Table 1).

As described in Figure 3, thiolutin stimulated Hsp27 phosphorylation in HUVEC required p38 but is not mediated through p38 activation. Further elucidation of the molecular mechanism for this response will be facilitated by this detailed characterization of site-specific Hsp27 phosphorylation. The role of the unique PTM in the N-terminus of Hsp27 in stress responses also remains to be defined.

Discussion

Based on previous isoelectric focusing studies, various cell types constitutively express 1 or 2 charge isoforms of Hsp27, but 2 to 4 additional charge isoforms of Hsp27 are rapidly induced in response to stress.[34–36] In these studies, metabolic labeling using $^{32}PO_4$ and IP with phospho-specific Hsp27 antibodies combined with phosphatase digestion demonstrated that several of the more acidic isoforms are phosphorylated. This result predicted that single and multiply phosphorylated isoforms of Hsp27 are induced by stress, but the specific sites phosphorylated could not be defined by such analysis, and other post-translational modifications that decrease the p*I* could not be excluded. Evaluating stress responses of human endothelial cells to the angiogenesis inhibitor thiolutin, we now demonstrate that multiple phosphorylation does occur, and the major diphosphorylated isoform of Hsp27 is modified at S78 and S82. At 60 min, pS82 is the most abundant monophosphorylated isoform, approximately 10-fold more abundant than pS78 by LC–MS analysis. This contrasts with the stronger immunoreactivity observed using a pS78 antibody and shows that comparing such signals between different phospho-specific antibodies can be misleading. Although immunoblotting indicated that S15 was transiently phosphorylated at earlier time points in response to thiolutin, by 60 min, LC–MS analysis established that pS15 accounts for less than 1% of Hsp27 phosphorylation. Therefore, triply phosphorylated Hsp27 is not a major species under these conditions. Furthermore, LC–MS analysis uncovered another major post-translational modification of Hsp27 that contributes to its observed charge heterogeneity. In human endothelial cells, we found that Hsp27 is essentially quantitatively modified by cleavage of the N-terminal Met and acetylation of the exposed subterminal Thr residue. The unmodified N-terminal sequence was essentially undetectable by LC–MS. This modification eliminates a positive charge at the N-terminus and so should decrease the pI of Hsp27. If this modification is not quantitative in other cell types, partial acetylation could explain the larger than expected number of charge isoforms of Hsp27 observed in some studies.[35,36] Acetylation could also potentially affect the oligomerization of Hsp27.

In this study, IP of Hsp27 combined with online LC–MS analysis was successfully employed to extensively characterize Hsp27 with a 100% sequence coverage. A very large Lys-C peptide fragment (a des-Met form with acetylation at the new N-terminus, 13 kDa) was identified with an optimized sample handling procedure prior to the LC–MS analysis. This large Lys-C peptide fragment was not observed initially in our LC–MS analysis. However, following addition of

the chaotropic reagent, 4 M guanidine hydrochloride (GnHCl), after the Lys-C digestion of Hsp27, the sample was loaded directly on an analytical C-8 column (to prevent potential losses in transfer from a precolumn to the separation column), and then washed with the mobile phase A for at least 2 h before gradient elution. This large Lys-C fragment (13 kDa) was then detected by FTICR MS. This sample handling procedure is critical regardless of the use of different types of analytical columns (i.e., C-4, C-8 or C-18). In addition, use of large pore size of reversed-phase packings (i.*e* ≥ 300 Å) further improved the recovery and peak shape of this large peptide, in agreement with our previous report.[26] Separately, we investigated several large fragments (4–15 kDa) from other proteins and found that the use of 4 M GnHCl also improved the recovery of these large peptides (data not shown). It should be noted that this sample handling procedure led to the removal of small or hydrophilic peptides during the long wash prior to the gradient elution. If necessary, these eluted peptides could be analyzed separately by injecting a sample without the addition of 4 M GnHCl. In addition to facilitating assignment of the phosphorylation sites, this approach permitted the identification of a previously unknown modification of the Hsp27 N-terminus. This structure could be difficult to obtain by traditional approaches because the hydrophobic nature at the N-terminal region of the molecule promotes oligomerization, thereby preventing the efficient enzymatic cleavage to obtain easily analyzed smaller fragments.

Since this large Lys-C peptide fragment of Hsp27 was not observed initially in our LC–MS analysis, we used a Lys-C plus Gluc-C fragment containing two phosphorylation sites, pS78 and pS82, for quantitation. Nevertheless, a very similar quantitation (%ES) using either the large Lys-C fragment or the Lys plus Gluc-C fragment was observed. Using the large Lys-C fragment, we could not detect any phosphorylation at S15 site. Only trace amounts of pS15, identified in a Lys-C plus trypsin fragment, could be found using a targeted LC–MS approach (SRM). It should also be noted that the Lys-C plus trypsin digest, similar to using trypsin alone, could identify pS82 but not pS78 because the trypsin cleavage rendered a fragment containing the pS78 site too small to be observed in LC–MS (see Figure 5). This pS78 could be overlooked by others using trypsin digest with a conventional LC–MS approach to study Hsp27.[37–39]

The specificity of the anti-pS78 antibody was evaluated by LC–MS analysis and revealed that the pS82 and doubly phosphorylated Hsp27 (pS78 plus pS82) were both immuno-precipitated by the anti-pS78 antibody. However, interpretation of the LC–MS data for the anti-pS78 antibody IP is limited if the phosphorylated Hsp27 is not monomeric. Recent sedimentation studies have shown that a phosphomimic mutant of Hsp27 retains the ability to form oligomers,[40] so we cannot exclude the possibility that anti-pS78 antibody actually pulled down singly S78 phosphorylated Hsp27 associated with oligomers containing multiply phosphorylated Hsp27.

Although thiolutin treatment preferentially induced JNK phosphorylation in HUVEC, downstream Hsp27 phosphorylation required p38 but not JNK activity (compare Figure 3C to B). Furthermore, JNK activation is not sufficient to activate the Hsp27 kinase MK2.[41] Therefore, thiolutin stimulation of Hsp27 phosphorylation requires p38 but is not mediated through activation of the p38 pathway. If JNK signaling plays any role in stimulation of Hsp27 phosphorylation by thiolutin, it may involve positive cross talk between the p38 and JNK pathways.[42] One such mechanism would involve thiolutin inhibiting a phosphatase that inactivates MK2 (see Row 2 in Figure 3A). The latter could be downstream or independent of JNK.

The combination of Western blotting, IP, and the LC–MS method described here enabled a sensitive quantitative characterization of PTMs and the stoichiometry of Hsp27 phosphorylation at multiple sites in the protein. These results set the stage for further study of the mechanism for regulation of Hsp27 phosphorylation in response to various stresses in many

cell types, and, in the context of endothelial cells, could provide new insights into the role of Hsp27 and MAP kinase signaling in controlling angiogenic responses. We are currently applying this LC–MS approach to quantitatively study the interaction partners of Hsp27 in endothelial cells and to assess the role of PTMs including phosphorylation on protein–protein interactions of Hsp27.

Abbreviations

ADT, 5-[*p*-methoxyphenyl]-3H-1,2-dithiol-3-thione; D3T, 1,2-dithiole 3-thione; FCS, fetal calf serum; Hsp27, heat shock protein 27; HUVEC, human umbilical vein endothelial cells.

Acknowledgment

We acknowledge support from NIH grant GM 15847 (BLK) and the Intramural Research Program of the NIH, NCI, Center for Cancer Research (D.D.R., D.A.W.). Contribution Number 925 from the Barnett Institute.

References

1. Landry J, Huot J. Regulation of Actin dynamics by stress-activated protein kinase 2 (SAPK2)-dependent phosphorylation of heat-shock protein of 27 kDa (Hsp27). Biochem. Soc. Symp 1999;64:79–89. [PubMed: 10207622]
2. Concannon CG, Gorman AM, Samali A. On the role of Hsp27 in regulating apoptosis. Apoptosis 2003;8(1):61–70. [PubMed: 12510153]
3. Arrigo AP. The cellular “networking” of mammalian Hsp27 and its functions in the control of protein folding, redox state and apoptosis. Adv. Exp. Med. Biol 2007;594:14–26. [PubMed: 17205671]
4. Huot J, Houle F, Marceau F, Landry J. Oxidative stress-induced Actin reorganization mediated by the p38 mitogen-activated protein kinase/heat shock protein 27 pathway in vascular endothelial cells. Circ. Res 1997;80(3):383–392. [PubMed: 9048659]
5. Lambert H, Charette SJ, Bernier AF, Guimond A, Landry J. HSP27 multimerization mediated by phosphorylation-sensitive intermolecular interactions at the amino terminus. J. Biol. Chem 1999;274 (14):9378–9385. [PubMed: 10092617]
6. Thériault JR, Lambert H, Chávez-Zobel AT, Charest G, Lavigne P, Landry J. Essential role of the NH2-terminal WD/EPF motif in the phosphorylation-activated protective function of mammalian Hsp27. J. Biol. Chem 2004;279(22):23463–23471. [PubMed: 15033973]
7. Lelj-Garolla B, Mauk AG. Self-association of a small heat shock protein. J. Mol. Biol 2005;345(3): 631–642. [PubMed: 15581903]
8. Pichon S, Bryckaert M, Berrou E. Control of Actin dynamics by p38 MAP kinase - Hsp27 distribution in the lamellipodium of smooth muscle cells. J. Cell Sci 2004;117(Pt 12):2569–2577. [PubMed: 15128872]
9. During RL, Gibson BG, Li W, Bishai EA, Sidhu GS, Landry J, Southwick FS. Anthrax lethal toxin paralyzes Actin-based motility by blocking Hsp27 phosphorylation. EMBO J 2007;26(9):2240–2250. [PubMed: 17446863]
10. Keezer SM, Ivie SE, Krutzsch HC, Tandle A, Libutti SK, Roberts DD. Angiogenesis inhibitors target the endothelial cell cytoskeleton through altered regulation of heat shock protein 27 and cofilin. Cancer Res 2003;63(19):6405–6412. [PubMed: 14559830]
11. Stokoe D, Engel K, Campbell DG, Cohen P, Gaestel M. Identification of MAPKAP kinase 2 as a major enzyme responsible for the phosphorylation of the small mammalian heat shock proteins. FEBS Lett 1992;313(3):307–313. [PubMed: 1332886]
12. New L, Jiang Y, Zhao M, Liu K, Zhu W, Flood LJ, Kato Y, Parry GC, Han J. PRAK, a novel protein kinase regulated by the p38 MAP kinase. EMBO J 1998;17(12):3372–3384. [PubMed: 9628874]
13. McLaughlin MM, Kumar S, McDonnell PC, Van Horn S, Lee JC, Livi GP, Young PR. Identification of mitogen-activated protein (MAP) kinase-activated protein kinase-3, a novel substrate of CSBP p38 MAP kinase. J. Biol. Chem 1996;271(14):8488–8492. [PubMed: 8626550]

14. Shi Y, Kotlyarov A, Laabeta K, Gruber AD, Butt E, Marcus K, Meyer HE, Friedrich A, Volk HD, Gaestel M. Elimination of protein kinase MK5/PRAK activity by targeted homologous recombination. Mol. Cell. Biol 2003;23(21):7732–7741. [PubMed: 14560018]
15. Rane MJ, Pan Y, Singh S, Powell DW, Wu R, Cummins T, Chen Q, McLeish KR, Klein JB. Heat shock protein 27 controls apoptosis by regulating Akt activation. J. Biol. Chem 2003;278(30):27828–27835. [PubMed: 12740362]
16. Zheng C, Lin Z, Zhao ZJ, Yang Y, Niu H, Shen X. MAPK-activated protein kinase-2 (MK2)-mediated formation and phosphorylation-regulated dissociation of the signal complex consisting of p38, MK2, Akt, and Hsp27. J. Biol. Chem 2006;281(48):37215–37226. [PubMed: 17015449]
17. Wu R, Kausar H, Johnson P, Montoya-Durango DE, Merchant M, Rane MJ. Hsp27 regulates Akt activation and poly-morphonuclear leukocyte apoptosis by scaffolding MK2 to Akt signal complex. J. Biol. Chem 2007;282(30):21598–21608. [PubMed: 17510053]
18. Döppler H, Storz P, Li J, Comb MJ, Toker A. A phosphorylation state-specific antibody recognizes Hsp27, a novel substrate of protein kinase D. J. Biol. Chem 2005;280(15):15013–15019. [PubMed: 15728188]
19. Butt E, Immler D, Meyer HE, Kotlyarov A, Laass K, Gaestel M. Heat shock protein 27 is a substrate of cGMP-dependent protein kinase in intact human platelets: phosphorylation-induced Actin polymerization caused by HSP27 mutants. J. Biol. Chem 2001;276(10):7108–7113. [PubMed: 11383510]
20. Bryantsev AL, Chechenova MB, Shelden EA. Recruitment of phosphorylated small heat shock protein Hsp27 to nuclear speckles without stress. Exp. Cell Res 2007;313(1):195–209. [PubMed: 17123510]
21. Bix G, Fu J, Gonzalez EM, Macro L, Barker A, Campbell S, Zutter MM, Santoro SA, Kim JK, Höök M, Reed CC, Iozzo RV. Endorepellin causes endothelial cell disassembly of Actin cytoskeleton and focal adhesions through alpha2beta1 integrin. J. Cell Biol 2004;166(1):97–109. [PubMed: 15240572]
22. Isenberg JS, Jia Y, Field L, Ridnour LA, Sparatore A, Del Soldato P, Sowers AL, Yeh GC, Moody TW, Wink DA, Ramchandran R, Roberts DD. Modulation of angiogenesis by dithiolethione-modified NSAIDs and valproic acid. Br. J. Pharmacol 2007;151(1):63–72. [PubMed: 17351657]
23. Celmer WD, Sobin BA. The isolation of two synergistic antibiotics from a single fermentation source. Antibiot. Annu 1955–1956;3:437–441. [PubMed: 13355307]
24. Minamiguchi K, Kumagai H, Masuda T, Kawada M, Ishizuka M, Takeuchi T. Thiolutin, an inhibitor of HUVEC adhesion to vitronectin, reduces paxillin in HUVECs and suppresses tumor cell-induced angiogenesis. Int. J. Cancer 2001;93(3):307–316. [PubMed: 11433393]
25. Wu SL, Kim J, Bandle RW, Liotta L, Petricoin E, Karger BL. Dynamic profiling of the post-translational modifications and interaction partners of epidermal growth factor receptor signaling after stimulation by epidermal growth factor using Extended Range Proteomic Analysis (ERPA). Mol. Cell. Proteomics 2006;5(9):1610–1627. [PubMed: 16799092]
26. Wu SL, Kim J, Hancock WS, Karger B. Extended Range Proteomic Analysis (ERPA): a new and sensitive LC–MS platform for high sequence coverage of complex proteins with extensive post-translational modifications-comprehensive analysis of beta-casein and epidermal growth factor receptor (EGFR). J. Proteome Res 2005;4(4):1155–1170. [PubMed: 16083266]
27. Zhang J, Wu SL, Kim J, Karger BL. Ultratrace liquid chromatography/mass spectrometry analysis of large peptides with post-translational modifications using narrow-bore poly(styrene-divinylbenzene) monolithic columns and extended range proteomic analysis. J. Chromatogr. A 2007;1154(1–2):295–307. [PubMed: 17442327]
28. Timmer JC, Enoksson M, Wildfang E, Zhu W, Igarashi Y, Denault JB, Ma Y, Dummitt B, Chang YH, Mast AE, Eroshkin A, Smith JW, Tao WA, Salvesen GS. Profiling constitutive proteolytic events in vivo. Biochem. J 2007;407(1):41–48. [PubMed: 17650073]
29. Johnson CA, White DA, Lavender JS, O'Neill LP, Turner BM. Human class I histone deacetylase complexes show enhanced catalytic activity in the presence of ATP and co-immunoprecipitate with the ATP-dependent chaperone protein Hsp70. J. Biol. Chem 2002;277(11):9590–9597. [PubMed: 11777905]
30. Perrier J, Durand A, Giardina T, Puigserver A. Catabolism of intracellular N-terminal acetylated proteins: involvement of acylpeptide hydrolase and acylase. Biochimie 2005;87(8):673–685. [PubMed: 15927344]

31. Reinders J, Wagner K, Zahedi RP, Stojanovski D, Eyrich B, van der Laan M, Rehling P, Sickmann A, Pfanner N, Meisinger C. Profiling Phosphoproteins of Yeast Mitochondria Reveals a Role of Phosphorylation in Assembly of the ATP Synthase. Mol. Cell. Proteomics 2007;6(11):1896–1906. [PubMed: 17761666]
32. Starling AP, Sharma RP, East JM, Lee AG. The effect of N-terminal acetylation on Ca(2+)-ATPase inhibition by phospholamban. Biochem. Biophys. Res. Commun 1996;226(2):352–355. [PubMed: 8806639]
33. Wagner BK, Kitami T, Gilbert TJ, Peck D, Ramanathan A, Schreiber SL, Golub TR, Mootha VK. Large-scale chemical dissection of mitochondrial function. Nat. Biotechnol 2008;26(3):343–351. [PubMed: 18297058]
34. Chrétien P, Landry J. Enhanced constitutive expression of the 27-kDa heat shock proteins in heat-resistant variants from Chinese hamster cells. J. Cell Physiol 1988;137(1):157–166. [PubMed: 3170655]
35. Landry J, Chrétien P, Lambert H, Hickey E, Weber LA. Heat shock resistance conferred by expression of the human HSP27 gene in rodent cells. J. Cell Biol 1989;109(1):7–15. [PubMed: 2745558]
36. Vanderwaal RP, Cha B, Moros EG, Roti Roti JL. HSP27 phosphorylation increases after 45 degrees C or 41 degrees C heat shocks but not after non-thermal TDMA or GSM exposures. Int. J. Hyperthermia 2006;22(6):507–519. [PubMed: 16971370]
37. Tremolada L, Magni F, Valsecchi C, Sarto C, Mocarelli P, Perego R, Cordani N, Favini P, Galli Kienle M, Sanchez JC, Hochstrasser DF, Corthals GL. Characterization of heat shock protein 27 phosphorylation sites in renal cell carcinoma. Proteomics 2005;5(3):788–795. [PubMed: 15682460]
38. Durán MC, Boeri-Erba E, Mohammed S, Martín-Ventura JL, Egido J, Vivanco F, Jensen ON. Characterization of HSP27 phosphorylation sites in human atherosclerotic plaque secretome. Methods Mol. Biol 2007;357:151–163. [PubMed: 17172686]
39. Huang SY, Tsai ML, Chen GY, Wu CJ, Chen SH. A systematic MS-based approach for identifying in vitro substrates of PKA and PKG in rat uteri. J. Proteome Res 2007;6(7):2674–2684. [PubMed: 17564427]
40. Somara S, Bitar KN. Tropomyosin interacts with phosphorylated HSP27 in agonist-induced contraction of smooth muscle. Am. J. Physiol. Cell Physiol 2004;286(6):C1290–C1301. [PubMed: 14749215]
41. Nickischer D, Laethem C, Trask OJ Jr, Williams RG, Kandasamy R, Johnston PA, Johnston PA. Development and implementation of three mitogen-activated protein kinase (MAPK) signaling pathway imaging assays to provide MAPK module selectivity profiling for kinase inhibitors: MK2-EGFP translocation, c-Jun, and ERK activation. Methods Enzymol 2006;414:389–418. [PubMed: 17110204]
42. Pimienta G, Pascual J. Canonical and alternative MAPK signaling. Cell Cycle 2007;6(21):2628. [PubMed: 17957138]

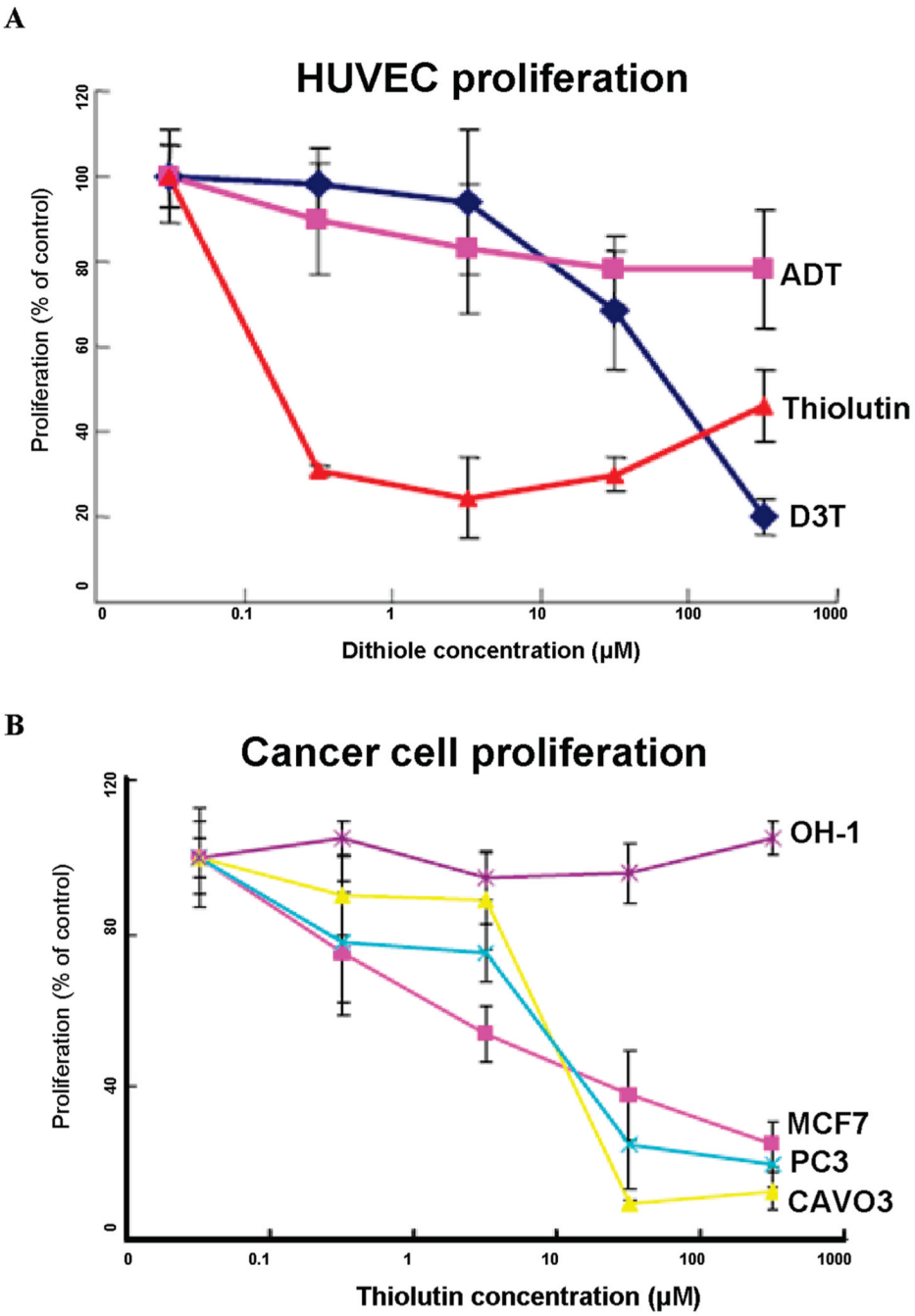

Figure 1.

Thiolutin selectively inhibits endothelial cell proliferation. (A) HUVEC (5000 cells/well) were plated on 96-well culture plates and incubated for 72 h in EGM + 2% FCS with the indicated treatment agents, Thiolutin, ADT (5-[*p*-methoxyphenyl]-3H-1,2-dithiol-3-thione), and D3T (1,2-dithiole 3-thione). Cell proliferation was assayed *via* the colorimetric change obtained after incubation with MTS reagent using a microplate reader at 490 nm. (B) Proliferation of breast carcinoma (MCF-7), prostate carcinoma (PC3), ovarian carcinoma (CaOV3), and small cell lung carcinoma (OH-1) cells was assessed in the presence of the indicated concentrations of thiolutin. Results are expressed as percentage of control and represent the mean ± SD of at least three separate experiments.

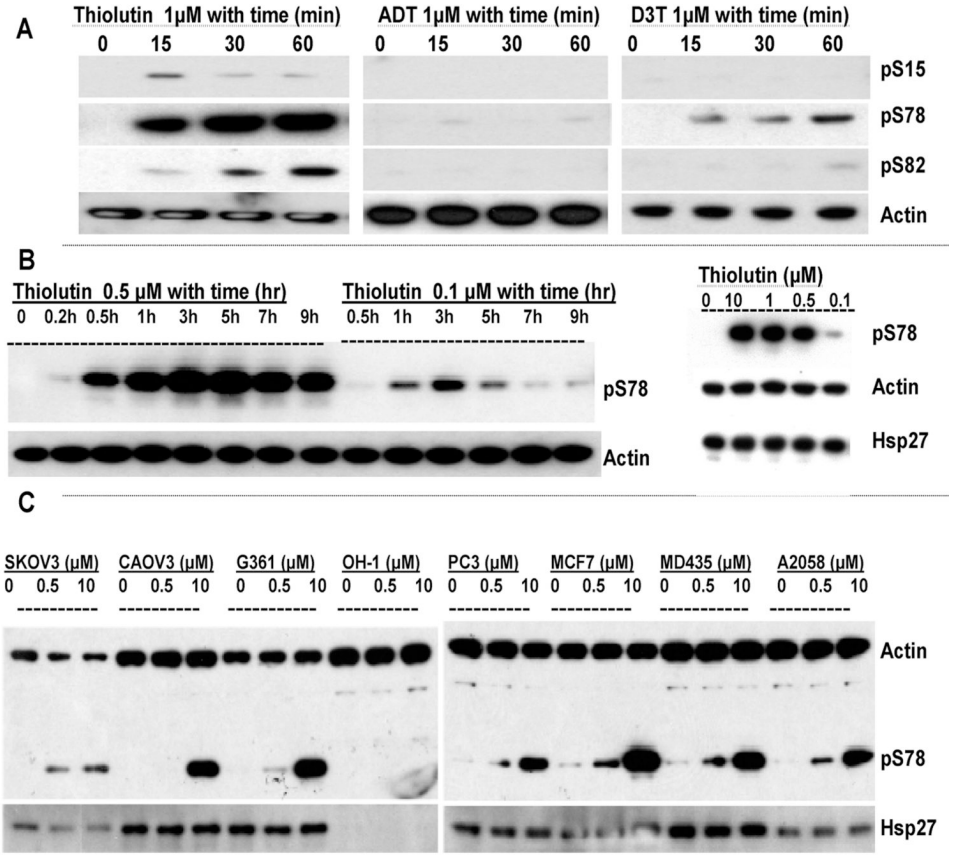

Figure 2.

Thiolutin selectively stimulates Hsp27 phosphorylation in endothelial cells. (A) HUVEC were treated with 1 μM of thiolutin, ADT, and D3T for the time indicated. Western blots were performed with anti-Hsp27 phosphorylation specific antibodies as described in Materials and Methods. The membranes were then reprobed with antiactin antibody for sample loading control. (B) HUVEC were treated with thiolutin at 0.5 or 0.1 μM for the time indicated. Right panel: HUVEC were treated with the indicated concentrations of thiolutin for 60 min. Samples were collected for Western blotting using anti-pS78 Hsp27, antiactin, and anti-Hsp27 antibodies. (C) Indicated tumor cell lines were treated with 0.5 or 10 μM thiolutin for 30 min. Cell lysates were analyzed by Western blotting probed with anti-Hsp27, anti-pS78 Hsp27, and antiactin antibodies.

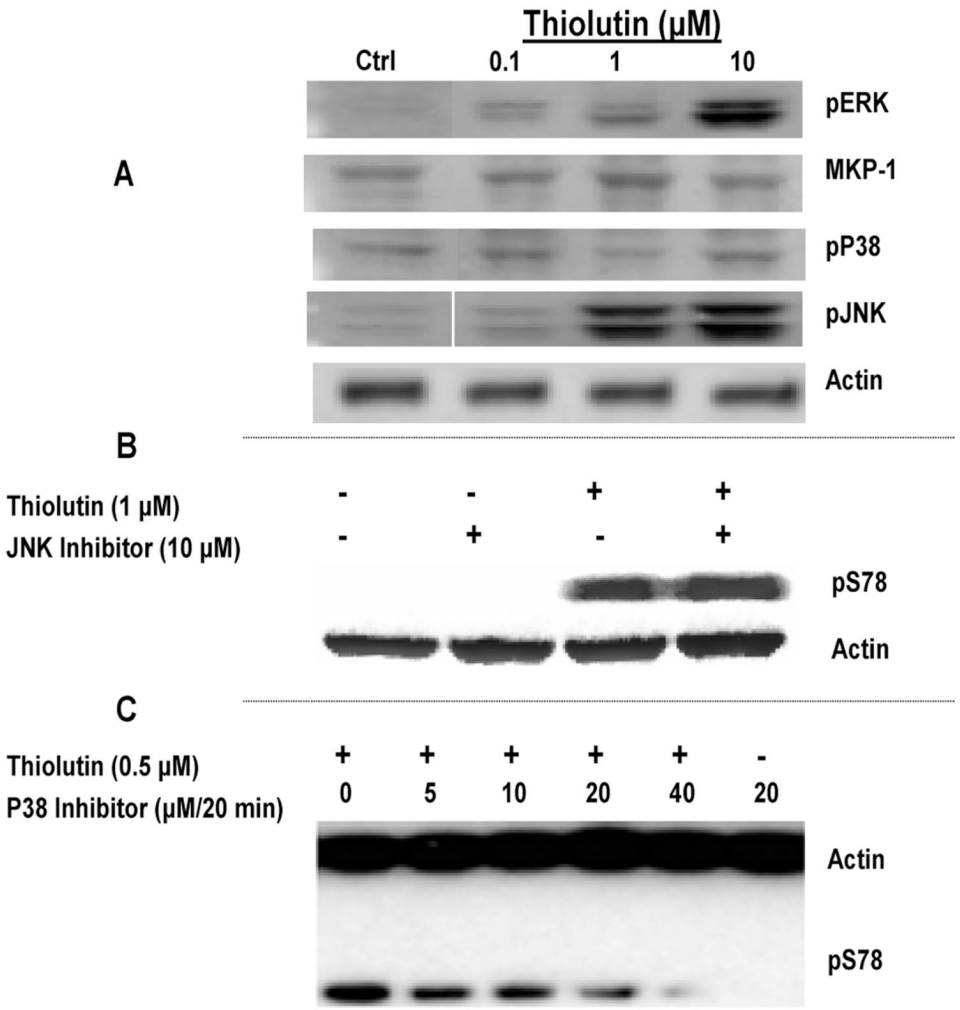

Figure 3.

p38 is required for Hsp27 phosphorylation but not activated by thiolutin. (A) Selective activation of MAP kinases by thiolutin. HUVEC were grown in full growth media, switched to EGM + 2% FBS for 24 h, and then treated with the indicated concentrations of thiolutin in EGM + 0.1% BSA. Lysates were analyzed by Western blots probed with antiphospho-ERK, phos-pho-JNK, or phospho-p38 antibodies. (B) HUVEC were treated with (+) or without (−) 10 μM of JNK inhibitor (SP600125) for 20 min followed with (+) or without (−) 1 μM thiolutin for 1 h. Samples were collected for Western blotting using anti-pS78 Hsp27 and antiactin antibodies. (C) HUVEC were treated with the indicated concentrations of the p38 inhibitor (SB203680) for 20 min and then treated with (+) or without (−) thiolutin at 0.5 μM for 1 h. Samples were collected for Western blotting using anti-pS78 Hsp27 and antiactin antibodies.

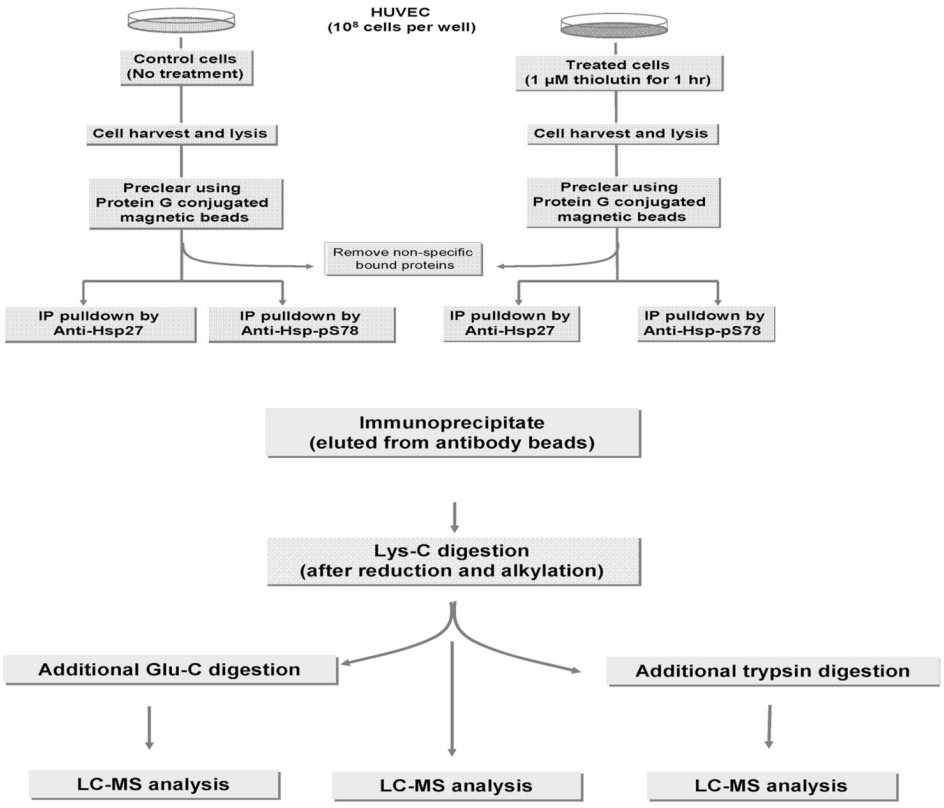

Figure 4.

(A) Workflow for the IP of Hsp27 from HUVEC. Each cell lysate (either treated with thiolutin at 1 μM for 60 min or without treatment) was IP by two different antibodies of HSP27, one against the backbone of the C-terminal end of Hsp27 and the other against phosphorylation at pS78 region. A total of four IPs were obtained for subsequent LC–MS analysis. (B) Workflow for LC–MS analysis. Each IP was first digested by Lys-C, and then one-third of the sample was further digested by trypsin and the other one thirds by Glu-C. Each digest (Lys-C plus trypsin or Lys-C plus Glu-C or Lys-C only) was subsequently analyzed by online LC–MS analysis.

Figure 5.

Summary of Hsp27 Peptides Identified by LC–MS Analysis. (A) The Hsp 27 peptides were identified from a Lys-C plus trypsin digested sample with the sequence coverage of 89.3% (amino acids in bold). (B) The Hsp 27 peptides were identified from the Lys-C plus Glu-C digested sample with the sequence coverage of 69.3% (amino acids in bold). The total sequence coverage was 96.1% when combining the identified peptides from the both digests. Fragments that contain the phosphorylation sites (S* in the figure) are underlined.

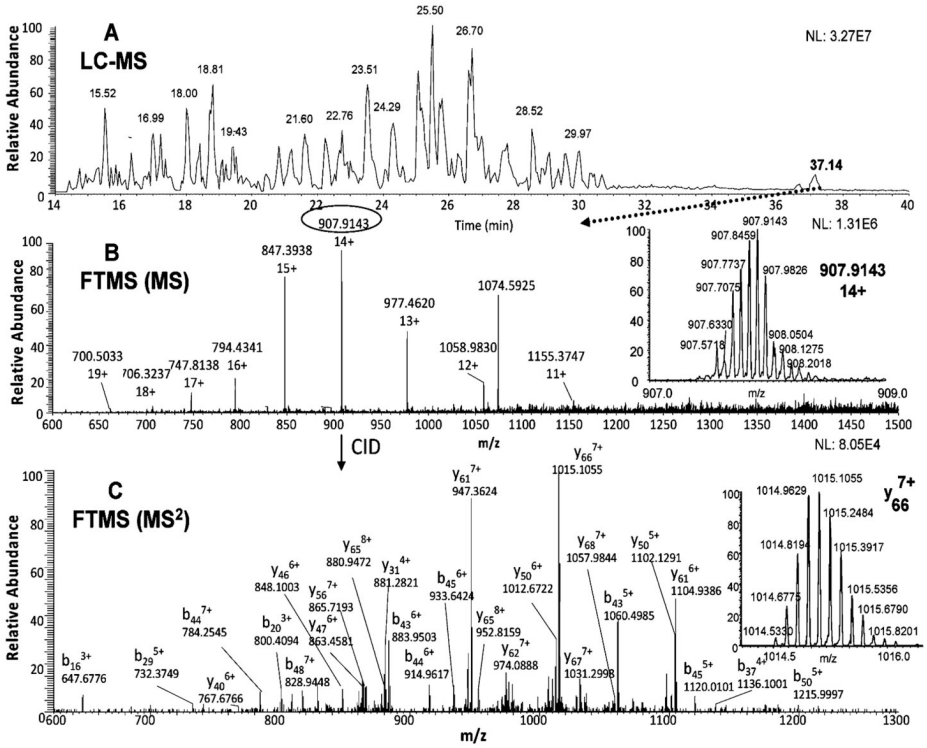

Figure 6.

Identification of acetylated species of the Lys-C fragment 2–112 of Hsp27 by LC–MS analysis. The base ion chromatogram of the Lys-C digest (A), the FTICR measurement of the precursor ion at 37.14 min with the ion of the highest charge state (14+ and *m*/*z* 907.9143) shown in the insert (B), the CID-MS^2 product ions of the precursor ion (*m*/*z* 907.9143) using the FTICR measurement with the highest product ion (y66, 7+) shown in the insert (C).

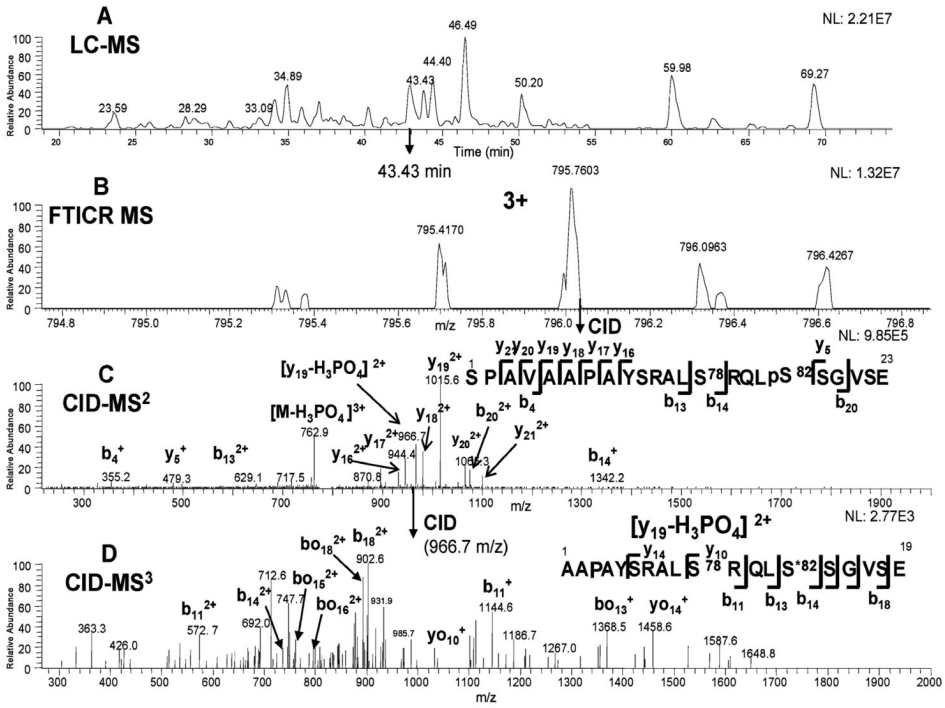

Figure 7.

Identification of the Glu-C fragment 65–87 of Hsp27 with pS82 by LC–MS analysis. The base ion chromatogram of the Lys-C plus Glu-C digest (A), the FTICR measurement of the precursor ion at 43.43 min (B), the CID-MS^2 product ions of the precursor ion (*m*/*z* 795.7603) at 43.43 min (C), and the CID-MS^3 product ions of the neutral loss ion (*m*/*z* 966.7) generated from the previous CID-MS2 fragmentation (D).

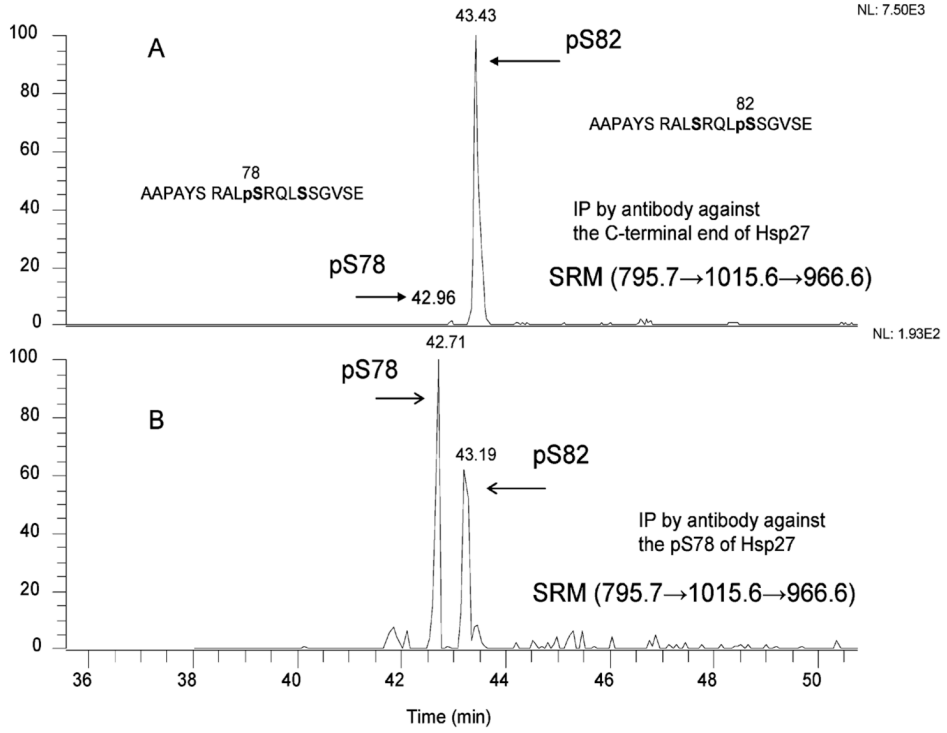

Figure 8.

Extracted ion chromatograms (XIC) of phosphorylated isoforms of the Glu-C fragment 65–87 of Hsp27. (A) Base peak XIC of the Glu-C fragment 65–87 of Hsp27 with monophosphorylation. The phosphorylated Hsp27, IP from the antibody against the C-terminal end, was indicated in the insert of (A). The extracted ion chromatogram (*m*/*z* 966.7) was isolated from the CID-MS^3 fragmentation, which was generated from the fragmentation of the ion (*m*/*z* 1015.6), and the 1015.6 ion was from the CID-MS^2 of the precursor ion (*m*/*z* 795.7). (B) Base peak XIC of the Glu-C fragment 65–87 of Hsp27 with monophosphorylation. The phosphorylated Hsp27, IP from the antibody against the pS78 region, was indicated in the insert of (B). The extracted ion chromatogram (*m*/*z* 966.7) was isolated from the same procedure as in (A).

Table 1

Estimated Stoichiometries (% ES) of pS78 and pS82 from IP of Hsp27 Before and After Thiolutin Treatment[a]

SPAVAAPAYSRALS(78)RQLS(82)SGVSE			
Groups	**No P**	**Mono P**	**Di-P (pS78+pS82)**
		IP using anti-Hsp27 Ab	
Control	100%	N.D.	N.D.
Thiolutin-treated	32%	47% at pS82 5% at pS78	16%
		IP using anti-pS78 Hsp27 Ab	
Control	N.D.	N.D.	N.D.
Thiolutin-treated	17%	10% at pS82 12% at pS78	61%

[a]The %ES was calculated as the measured phosphopeptide divided by the sum of the same peptide with various forms. N.D. means not detected.